

Changes to the extreme and erratic behaviour of cryptocurrencies during COVID-19

Nick James^a, Max Menzies^b, Jennifer Chan^a

^a*School of Mathematics and Statistics, University of Sydney, NSW, Australia*

^b*Yau Mathematical Sciences Center, Tsinghua University, Beijing, China*

Abstract

This paper introduces new methods for analysing the extreme and erratic behaviour of time series to evaluate the impact of COVID-19 on cryptocurrency market dynamics. Across 51 cryptocurrencies, we examine extreme behaviour through a study of distribution extremities, and erratic behaviour through structural breaks. First, we analyse the structure of the market as a whole and observe a reduction in self-similarity as a result of COVID-19, particularly with respect to structural breaks in variance. Second, we compare and contrast these two behaviours, and identify individual anomalous cryptocurrencies. USDT and TUSD are consistent outliers with respect to their returns, while HOT, NEXO, MKR and XEM are frequently observed as anomalous with respect to both behaviours and time. Even among a market known as consistently volatile, this identifies individual cryptocurrencies that behave most irregularly in their extreme and erratic behaviour and shows these were more affected during the COVID-19 market crisis.

Keywords: COVID-19, cryptocurrencies, time series, change-point detection, anomaly detection, nonlinear dynamics

1. Introduction

The COVID-19 pandemic has had immense impacts on society, and prompted a substantial amount of attention and research. Epidemiologists have studied the spread of COVID-19 and potential measures of containment [1, 2, 3, 4, 5, 6] and medical researchers are urgently investigating treatments for the disease [7, 8, 9, 10, 11, 12] and developing a vaccine [13]. Within the nonlinear dynamics community, applied mathematicians have used new and traditional techniques to analyse and predict the spread evolution of COVID-19 cases and deaths in a wide breadth of research [14, 15, 16, 17, 18, 19]. A limited amount of research has used standard statistical methods [20] and parametric models [21, 22] to study the impact of COVID-19 on financial markets, and the cryptocurrency market in particular [23].

Well before the pandemic, cryptocurrencies have been of great interest to researchers in dynamical systems and econophysics. There has been substantial

research on individual cryptocurrencies such as Bitcoin [24, 25, 26, 27, 28] and the disorder and fractal behaviour within cryptocurrencies in general [29, 30, 31, 32]. Structural breaks of cryptocurrencies have been analysed in [33, 34], who imply, but do not explicitly state, that structural breaks, namely points in time where statistical properties change, herald erratic and unpredictable behaviour.

The goal of this paper is to extend the study of the nonlinear dynamics of cryptocurrencies and introduce new methods to analyse their extreme and erratic behaviour. Extreme behaviour is analysed via distributions that capture the extremal values of the log returns and Parkinson variance time series; erratic behaviour is analysed via structural breaks. We build on the existing literature in several ways. While [23] studies the impact of COVID-19 on 5 cryptocurrencies and [33] studies the structural breaks of 7 cryptocurrencies, we analyse the impact of COVID-19 on the extreme behaviour and structural breaks of 51 cryptocurrencies. We identify changes due to market dynamics in general, and identify numerous specific cryptocurrencies that are anomalous with respect to returns or variance. Further, we develop new *inconsistency matrices* to compare the relationship between extreme and erratic behaviours, which does not exist in the literature, before and after the emergence of COVID-19.

In Section 2, we describe our methodology to analyse extreme and erratic behaviour of an arbitrary collection of time series. The methods there are more general than this particular application. In Section 3, we apply our methods to the log returns and Parkinson variance time series for 51 cryptocurrencies. We conclude in Section 4.

2. Methodology

In this paper, the most general object of study is a collection of real-valued time series $X_t^{(i)}, i = 1, \dots, n$ over a time interval $t = 1, \dots, T$. We analyse four such collections: the log returns and Parkinson variance of 51 cryptocurrencies before and during the COVID-19 pandemic. At time t , let P_t, H_t, L_t be the adjusted closing price, the daily high, and the daily low, respectively, of a financial instrument at time t . Let R_t and σ_t be the log returns and Parkinson variance time series, respectively, defined as

$$R_t = \log \left(\frac{P_t}{P_{t-1}} \right) \quad (1)$$

$$\sigma_t = \frac{(\log H_t - \log L_t)^2}{4 \log 2} \quad (2)$$

R_t takes both positive and negative values, while σ_t is non-negative everywhere, a distinction that is necessary in Section 2.1. The precise methodology that we describe below is not exhaustive. As long as there is consistency between the time series of interest, the change point algorithm, and the distance metric between distributions, the method below could easily be reworked for general use to other time series and data sets, both arbitrary and non-negative everywhere. Below we outline the detailed implementation to model the erratic and extreme

behaviour of cryptocurrencies. The choices of the Mann-Whitney test and the Wasserstein metric between distributions are natural choices in this context.

2.1. Distance between extreme values

In this section, we describe how we extract and measure distance between the extremal values of various time series. Let μ be a probability distribution that records the values of a time series X_t . For full generality, suppose μ is a continuous probability measure of the form $\mu = f(x)dx$, where dx is Lebesgue measure, and $f(x)$ a probability density function. As such, $f(x)$ is non-negative everywhere with integral 1.

For the log return time series R_t , we extract the points of density 5% and 95% respectively by the equations

$$\int_{-\infty}^s f(x)dx = 0.05 \quad (3)$$

$$\int_t^{\infty} f(x)dx = 0.05 \quad (4)$$

The range $x \leq s$ gives the left extremal 5% of the distribution, while the range $x \geq t$ gives the right extremal 5%. Next, we define the restricted function by

$$g(x) = f(x) \mathbb{1}_{\{x \leq s\} \cup \{x \geq t\}} = \begin{cases} f(x), & x \leq s \\ 0, & s < x < t \\ f(x), & x \geq t \end{cases} \quad (5)$$

Above, $\mathbb{1}$ denotes an indicator function of a set; this construction essentially truncates f only in its tail range. Next, we form the associated Radon-Nikodym measure $\nu = g(x)dx$, where dx is Lebesgue measure.

For the Parkinson variance time series σ_t , the associated function f is supported on $(0, \infty)$. In this case, we extract the point of density 90% by

$$\int_l^{\infty} f(x)dx = 0.10 \quad (6)$$

In this instance, we truncate f only in its extremal positive range by defining

$$h(x) = f(x) \mathbb{1}_{\{x \geq l\}} = \begin{cases} f(x), & x \geq l \\ 0, & x < l \end{cases}$$

Again, we form the Radon-Nikodym measure $\eta = h(x)dx$ where dx is Lebesgue measure. In both cases, this procedure works even more simply for a discrete distribution given by a finite data set. For the log returns, we simply form the empirical distribution function, then removes the middle 90% of the values by order; for the Parkinson variance, we remove the bottom 90% of the values.

Now suppose we are given n time series $X_t^{(i)}, i = 1, \dots, n$. We form n associated probability measures μ_1, \dots, μ_n and then the restricted measures ν_1, \dots, ν_n in the general case and η_1, \dots, η_n in the non-negative case. All these restricted measures have total measure equal to 0.1 so we may form Wasserstein distances [35] between them. We conclude by forming a matrix between the extreme values of the time series. Let $D_{ij}^{ER} = d_W(\nu_i, \nu_j)$ be the matrix between the log return distributions, and $D_{ij}^{EV} = d_W(\eta_i, \eta_j)$ be the matrix between the Parkinson variance distributions.

Finally, in Section 3 we will consider the mean $\mathbb{E}(\nu_i)$ of any restricted distribution associated to the log returns. Its sign reveals whether extreme positive or negative returns are more significant on average.

2.2. Distance between erratic behaviour profiles

Let X_t be a time series, $t = 1, \dots, T$. We apply the two-phase change point detection algorithm described by [36] to obtain a set of structural breaks. Applied to a collection $X_t^{(i)}, i = 1, \dots, n$ of time series, this produces a collection of finite sets S_1, \dots, S_n .

Next, we measure appropriate distances between the sets S_i . Traditional metrics such as the Hausdorff distance are unsuitable, being too sensitive to outliers [37] so we adopt and modify the semi-metrics developed in [34] between the sets of structural breaks S_i . We define a normalised distance by:

$$D(S_i, S_j) = \frac{1}{2T} \left(\frac{\sum_{b \in S_j} d(b, S_i)}{|S_j|} + \frac{\sum_{a \in S_i} d(a, S_j)}{|S_i|} \right) \quad (7)$$

This is a L^1 norm average of all minimal distances $d(a, S_2)$ from elements of S_1 to S_2 and vice versa, normalised by both the size of the sets and the length of the time series. As in Section 2.1, we form a matrix between the sets of structural breaks, $D_{ij}^B = D(S_i, S_j)$. Let D^{BR} and D^{BV} be the matrices between sets of structural breaks for the log return and Parkinson variance time series respectively.

2.3. Time-varying dynamics of the cryptocurrency market

In this section, we describe how we analyse the dynamics of returns and variance across the entire cryptocurrency market, before and after COVID-19. Let the Frobenius norm of a vector $v \in \mathbb{R}^n$ and an $n \times n$ matrix A be defined as $\|v\| = (\sum_{i=1}^n |v_i|^2)^{\frac{1}{2}}$ and $\|A\| = (\sum_{i,j=1}^n |a_{ij}|^2)^{\frac{1}{2}}$, respectively. At each time t , let \mathbf{R}_t and Σ_t be the length n vectors of all log returns ($R_t^{(i)}$) and Parkinson variances ($\sigma_t^{(i)}$) at time t , respectively. We study the change of the values $\|\mathbf{R}_t\|$ and $\|\Sigma_t\|$ over time as a proxy for the total volatility in the market. They determine the magnitude of absolute returns and Parkinson variance, respectively, and highlight the evolution of the spread in the first two distribution moments across the entire market. Having studied overall market dynamics, we next seek to understand the changing relationships between cryptocurrencies. For this

purpose, we study four different time series consisting of the log returns and Parkinson variance over two different periods, and compare the distance matrices we have defined, that is, pertaining to return breaks, return extremes, variance breaks and variance extremes. We study the magnitude of the respective matrix norms pre- and post-COVID-19 to understand the pandemic’s impact on the similarity and dynamics of the cryptocurrency market. Our time periods of analysis are 30-06-2018 to 31-12-2019 as “pre-COVID-19,” which we denote with the subscript “pre” and 1-1-2020 to 24-06-2020 as “post-COVID-19,” which we denote with the subscript “post.” Then, we have 8 different distance matrices:

- For the log returns pre-COVID time series, we have D_{pre}^{BR} and D_{pre}^{ER} ;
- For the Parkinson variance pre-COVID time series, have D_{pre}^{BV} and D_{pre}^{EV} ;
- For the log returns post-COVID time series, have D_{post}^{BR} and D_{post}^{ER} ;
- For the Parkinson variance post-COVID time series, have D_{post}^{BV} and D_{post}^{EV} .

We compute the Frobenius norms for these 8 matrices in Section 3.

2.4. Cross-contextual analysis

In this section, we describe how we measure the consistency between the extreme and erratic behaviours of cryptocurrencies. To do so, we introduce a new method of comparing distance matrices and then apply this to compare D^B and D^E for both the log return and Parkinson variance time series.

Given an $n \times n$ distance matrix A , the *affinity matrix* is defined as

$$A_{ij} = 1 - \frac{D_{ij}}{\max\{D\}}, \quad (8)$$

All elements of these affinity matrices lie in $[0, 1]$ so it is appropriate to compare them directly by taking their difference. Let the affinity matrices associated to D^{BR}, D^{BV} , defined in Section 2.2, and D^{ER}, E^{EV} , defined in Section 2.1, be $A^{BR}, A^{BV}, A^{ER}, A^{EV}$ respectively. Let the *inconsistency matrix* between extreme and erratic behaviour be defined as follows, for log returns and Parkinson variance respectively

$$\text{INC}^{R,EB} = A^{ER} - A^{BR} \quad (9)$$

$$\text{INC}^{V,EB} = A^{EV} - A^{BV} \quad (10)$$

As described in Section 2.3, we analyse the log returns and Parkinson variances over two distinct periods (pre- and post-COVID-19), so we have four different behaviour inconsistency matrices $\text{INC}_{\text{pre}}^{R,EB}, \text{INC}_{\text{pre}}^{V,EB}, \text{INC}_{\text{post}}^{R,EB}, \text{INC}_{\text{post}}^{V,EB}$.

Finally, we can also define inconsistency matrices with respect to time. By comparing corresponding distances matrices, extreme or erratic, over time, we can continue the goal of Section 2.3 and identify individual cryptocurrencies that

have significantly changed with respect to their similarity with others. Define four inconsistency matrices with respect to time:

$$\text{INC}_{\text{time}}^{ER} = A_{\text{pre}}^{ER} - A_{\text{post}}^{ER} \quad (11)$$

$$\text{INC}_{\text{time}}^{EV} = A_{\text{pre}}^{EV} - A_{\text{post}}^{EV} \quad (12)$$

$$\text{INC}_{\text{time}}^{BR} = A_{\text{pre}}^{BR} - A_{\text{post}}^{BR} \quad (13)$$

$$\text{INC}_{\text{time}}^{BV} = A_{\text{pre}}^{BV} - A_{\text{post}}^{BV} \quad (14)$$

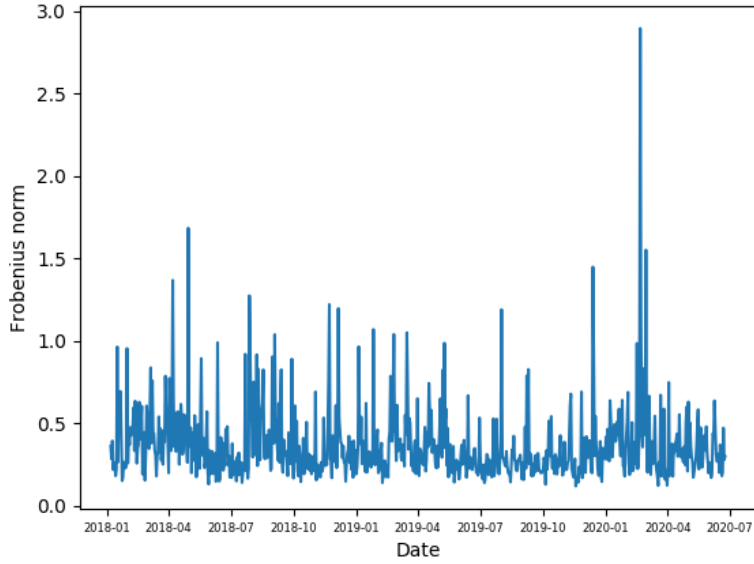
Let the *anomaly score* associated to any inconsistency matrix of any individual cryptocurrency be defined as $a_j = \sum_{j=1}^n |\text{INC}_{ij}|$. Larger values indicate cryptocurrencies that are more anomalous between the two behaviours under consideration. In Section 3, we rank the top 3 cryptocurrencies across a range of inconsistencies to determine the most prominent anomalies.

3. Experimental results and discussion

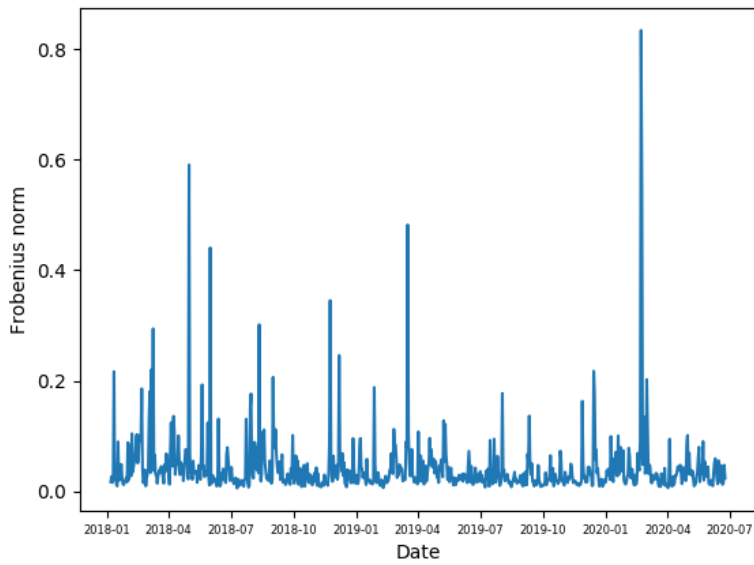
We draw data from Coinmarketcap. Of the cryptocurrencies with price histories that go as far back as 30-06-2018, we analyse the 51 largest by market capitalisation. For each cryptocurrency, we draw adjusted closing price, daily high, and daily low, and first calculate the log returns and Parkinson variance as defined in (1) and (2). In the proceeding sections, we report a broad range of findings with respect to the contrasting impact COVID-19 has had on the extreme and erratic behaviour of the cryptocurrency market’s returns and variance, the identification of inconsistencies in various cryptocurrency behaviours. We refer to the period from 30-06-2018 to 31-12-2019 as “pre-COVID-19” and the period from 1-1-2020 to 24-06-2020 as “post-COVID-19.”

3.1. COVID-19 impact on market dynamics

In this first section, we study the cryptocurrency market dynamics over time as a whole, without reference to the internal similarity between distinct cryptocurrencies. In Figures 1a and 1b, we depict the Frobenius norms $\|\mathbf{R}_t\|$ and $\|\Sigma_t\|$, respectively, defined in Section 2.3. Larger magnitudes indicate more unstable market dynamics, characterised by more total returns and variance (regardless of direction). These figures reveal several insights: first, during 2018 and 2019, the Parkinson variance exhibits less regular peaks than the log returns, but relative to the mean these peaks are more significant. These peaks also appear to occur more periodically than that of returns, with our measure possibly highlighting some latent volatility clustering. Second, the sharpest peak of each figure is coincident: anomalously large changes in returns are accompanied by proportionally large changes in variance at the same time. It appears the greatest impact of COVID-19 is felt at a single point in March. Third, after this greatest spike, both measures drop to levels below their 30 month average. That is, after this point, the volatility of the market is actually reduced relative to the previous year.



(a) The Frobenius norm $\|\mathbf{R}_t\|$ as a function of time



(b) The Frobenius norm $\|\Sigma_t\|$ as a function of time

Figure 1: The changing dynamics of the Frobenius norm for (a) log returns and (b) Parkinson variance over the whole market are plotted with time. A coincident sharp peak in March 2020 can be seen, showing the extreme but brief impact of COVID-19.

Matrix norms $\ D^E\ $ for returns and variance, pre- and post-COVID-19		
Period	Log returns	Parkinson variance
Pre-COVID-19	1.30	0.64
Post-COVID-19	1.51	0.73

Table 1: Frobenius norms for extreme value distance matrices pre- and post-COVID-19.

Matrix norms $\ D^B\ $ for returns and variance, pre- and post-COVID-19		
Period	Log returns	Parkinson variance
Pre-COVID-19	5.70	0.84
Post-COVID-19	5.22	2.44

Table 2: Frobenius norms for structural breaks distance matrices pre- and post-COVID-19.

3.2. Changing dynamics of extreme and erratic behaviour

In this section, we analyse the distance matrices between structural breaks and extreme values pertaining to the four time series under consideration, that is, log returns and Parkinson variance before and after the emergence of COVID-19. First, both before and after the emergence of COVID-19, the behaviour of cryptocurrencies is more self-similar with respect to variance than returns. This is true for both extreme values and structural breaks, heralding extreme and erratic behaviour, respectively. This can be seen in the consistently smaller values in Tables 1 and 2, where Frobenius norms, defined in Section 2.3 as computed. All distances in question, and hence the matrix norms, are normalised, so this comparison is appropriate when comparing extreme values or structural breaks over the same period between returns and variance.

Next, the post-COVID-19 period has generally exhibited less similarity in the cryptocurrency period than the prior period. Comparing extreme values and structural breaks with respect to the log returns and variance time series, three of these distance matrices exhibit greater Frobenius norm for the post-COVID-19 period. Only the structural breaks with respect to returns observe a slight decrease in Frobenius norm, heralding greater self-similarity, in the post-COVID-19 period. By contrast, the Frobenius norm for breaks with respect to variance has increased almost threefold. Indeed, this can be seen in Figure 2. As we will discuss further in Section 3.3, Figure 2a shows essentially one cluster, broad self-similarity and no anomalous elements between structural breaks with respect to variance, while Figure 2b has less similarity and several anomalous elements.

On the other hand, for the Frobenius norms with respect to extreme values, a moderate and similar increase was observed for both returns and variance. That is, the total similarity in return and variance extremes decreased by a similar amount due to COVID-19. The slight increase in Frobenius norm for extreme values of variance contrasts with the large increase in the case of breaks; while the increase in norms for log returns contrasts with the decrease in the case of structural breaks.

3.3. Structural breaks with respect to Parkinson variance

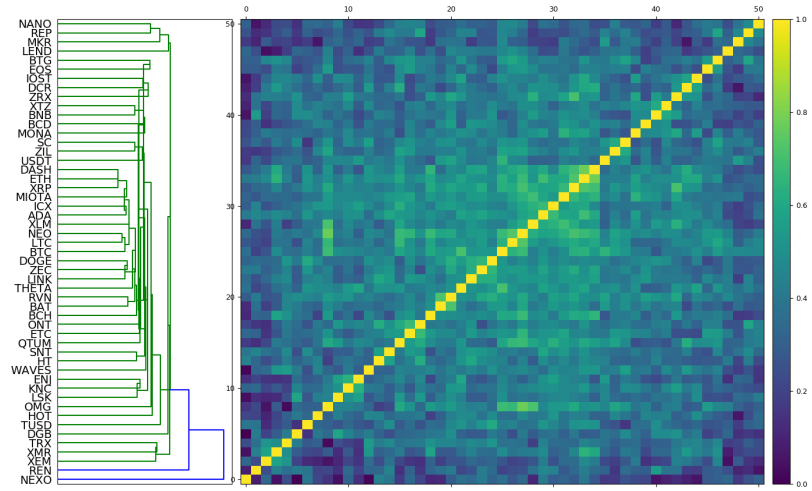
In this section, we take a closer look at the structure of the cryptocurrency market with respect to structural breaks in Parkinson variance. In Figure 2, we depict the results of hierarchical clustering of the distance matrix between structural breaks with respect to variance. This supports our analysis in the preceding section. Figure 2a exhibits essentially one cluster, with no notable anomalies and a high degree of self-similarity. This complete lack of individual subclusters represents the significant risk for investors in the cryptocurrency market as a whole: there is really no way to diversify against erratic behaviour with respect to volatility, as all cryptocurrencies have highly similar structural breaks. This will likely cause substantial risk of drawdowns among a collection of cryptocurrencies. In Figure 2b, two primary clusters of cryptocurrencies are observed. Within the smaller cluster, a subcluster of high similarity emerges containing cryptocurrencies such as ETH and XMR. All individual cryptocurrency tickers are labelled in Table A.3.

3.4. Extreme values with respect to log returns

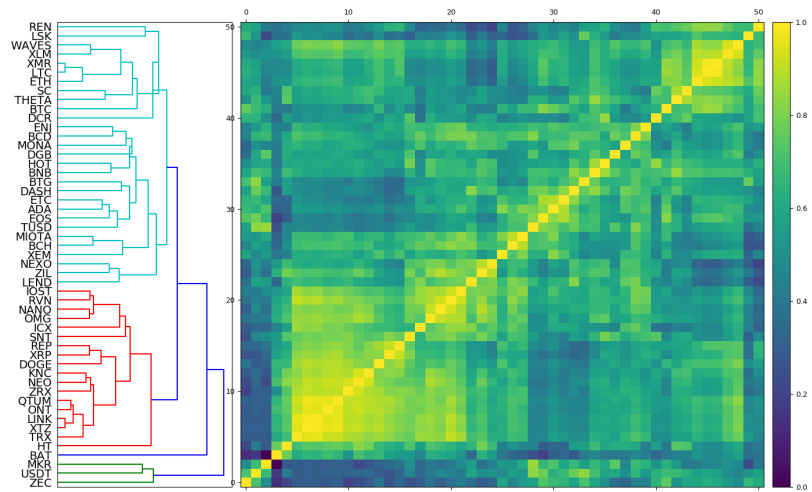
In this section, we analyse the impact of COVID-19 on the extreme values of the log returns. Analysis of the distances between these extremal distributions reveals more pronounced structure forming after the emergence of COVID-19. Figures 3a and 3b display hierarchical clustering on the matrix D^{ER} pre- and post-COVID-19. These dendrograms highlight one large predominant cluster containing all but two cryptocurrencies, and an anomalous cluster containing only USDT and TUSD, consistent pre- and post-COVID-19. Both these cryptocurrencies are highly anomalous with respect to their log returns, likely due to their oddly thin trading structure and limited range in their price movements. Indeed, in Figure 4, we depict the extremal distributions of their log returns alongside cryptocurrencies in the majority cluster, BTC and ETH. Comparing Figures 4a and 4b with Figures 4c and 4d, we see almost a tenfold difference in scale in the log returns. Similar behaviour exists after the emergence of COVID-19 in Figures 4e, 4f, 4g and 4h. Moreover, USDT and TUSD's distributions in 4e and 4f, respectively, lack the asymmetry and negative skew observed for BTC and ETH in 4g and 4h. The distributions of BTC and ETH, which are representative of the extreme return behaviours of most cryptocurrencies, highlight the pronounced negative skew such securities experience during times of market crisis.

With this in mind, we treat USDT and TUSD as outliers and analyse the collection after removing them. Figure 3c determines four distinct clusters, two of which contain the majority of cryptocurrencies. In Figure 3d, which depicts the post-COVID-19 period, all but two cryptocurrencies, LEND and DGB, belong to one dominant cluster. The difference in the number of clusters and structure of these dendrograms highlights the significant impact COVID-19 has had on extreme return behaviours.

Next, we take a closer look at the cluster structure of the return extremes, particularly with respect to the means of the restricted distributions, as defined



(a) D_{pre}^{BV} dendrogram



(b) D_{post}^{BV} dendrogram

Figure 2: Hierarchical clustering of distance matrix between structural breaks with respect to Parkinson variance for (a) pre-COVID-19 and (b) post-COVID-19.

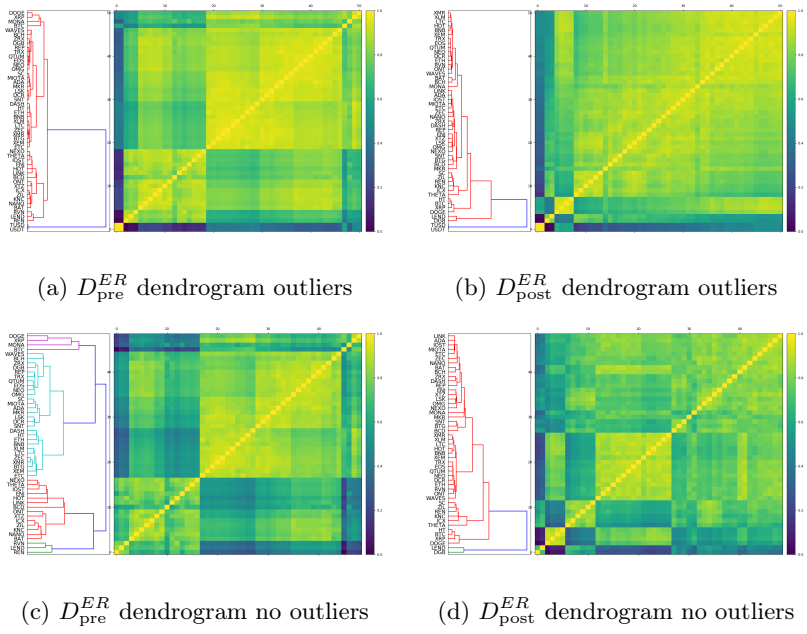


Figure 3: Hierarchical clustering of distance matrix between extreme values with respect to log returns for (a) pre-COVID-19, (b) post-COVID-19 and without outliers USDT and TUSD, (c) pre-COVID-19 and (d) post-COVID-19.

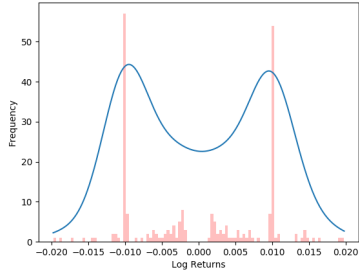
in Section 2.1. We see that the means have a significant relationship with the cluster structure in both periods:

1. Before COVID-19, Figure 3c identifies four distinct clusters. However, after inspection of the dendrogram and Figure 3a, we see that these four naturally fit into two larger clusters: one containing BTC, ETH among others, and one containing HOT and LEND, among others. Computing the means of these two clusters reveals a meaningful relationship: the four largest values of $\mathbb{E}(\nu_i)$ all lie in the second cluster, and the mean of the means $\mathbb{E}_i \mathbb{E}(\nu_i)$ is greater than the mean of the first cluster under a simple statistical test, $p < 0.05$.
2. Post-COVID-19, excluding outliers USDT and TUSD, the two anomalous cryptocurrencies LEND and DGB have the two largest means $\mathbb{E}(\nu_i)$ of the entire post-COVID-19 collection.
3. Pre-COVID-19, 88% of cryptocurrencies had an negative value of $\mathbb{E}(\nu_i)$. Post-COVID-19, 37% of cryptocurrencies had a negative valued mean. That is, a majority of post-COVID-19 return extremes had a positive mean. This is a surprising result and demonstrates that although there was a sharp initial drop in returns due to COVID-19, this behaviour was anomalous across the post-COVID-19 period as a whole.

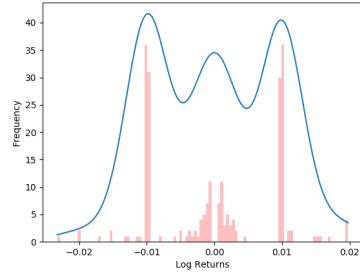
3.5. Identification of cryptocurrency anomalies

In this section, we focus on identifying two types of anomalies within the cryptocurrency market - cryptocurrencies that are inconsistent between extreme and erratic behaviour, or inconsistent with respect to time.

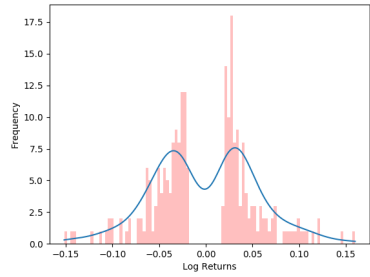
Inconsistencies with respect to behaviour are analysed through the inconsistency matrices $\text{INC}_{\text{pre}}^{R,EB}$, $\text{INC}_{\text{pre}}^{V,EB}$, $\text{INC}_{\text{post}}^{R,EB}$, $\text{INC}_{\text{post}}^{V,EB}$ and anomaly scores defined in Section 2.4. We implement hierarchical clustering in Figure 5 to highlight clusters in returns and variance, and compute anomaly scores. The inconsistency dendrogram with respect to pre-COVID-19 returns is displayed in Figure 5a and reveals a separate cluster of HOT, ZRX and LEND. Computing anomaly scores reveals the top three most inconsistent cryptocurrencies with respect to differing behaviour features to be HOT, ZRX and MKR - LEND is fourth. The anomaly scores may give slightly different results than the hierarchical clustering: the anomaly scores feature absolute values to calculate absolute differences with all other elements, while the dendrograms cluster based on the positive or negative values of the inconsistency matrix. Several negative rows may indicate cryptocurrencies of similar behaviour that should be clustered together, but might not necessarily distinguish the most absolutely anomalous entries of the collection. The behaviour inconsistency matrix with respect to post-COVID-19 returns is clustered in Figure 5b. NEXO, USDT and TUSD form their own cluster; the top 3 anomaly scores are of NEXO, THETA and MKR.



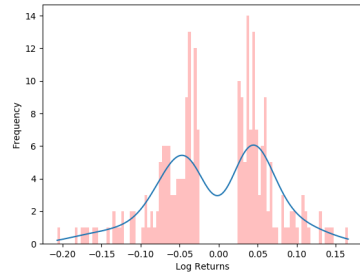
(a) USDT



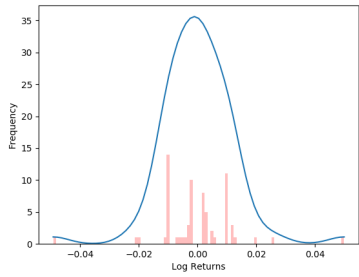
(b) TUSD



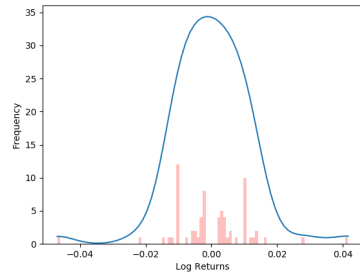
(c) BTC



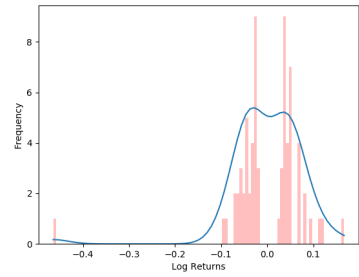
(d) ETH



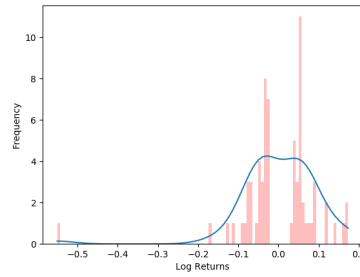
(e) USDT



(f) TUSD



(g) BTC



(h) ETH

Figure 4: Extreme values of log returns distributions. Figures (a)-(d) represent pre-COVID-19 distributions, (e)-(h) represent post-COVID-19 distributions.

When analysing inconsistency matrices between extreme and erratic behaviour of variance, we observe repetition of anomalous cryptocurrencies - the top 3 anomaly scores for the pre-COVID-19 variance behaviour inconsistency matrix are XEM, NEXO and MKR. When observing the dendrograms in Figures 5c and 5d side by side, slightly more structure is observed in the post-COVID-19 period, with a growth in the total number of clusters. USDT and TUSD emerge as inconsistent in their behaviour after the emergence of COVID-19. Indeed, pre-COVID-19, both their extreme values and structural breaks are anomalous, leading to low inconsistency between the two behaviours, while post-COVID-19, their structural breaks in variance become similar to the rest of the market.

Time inconsistencies are analysed in Figure 6, where the time inconsistency matrices are clustered to highlight inconsistencies. Dendrograms for returns and variance extremes are dominated by one cluster - with each inconsistency matrix producing one anomalous cryptocurrency, DGB and BCD respectively. Indeed, these cryptocurrencies are each the highest anomaly score for returns and variance extremes, respectively. Several anomalous cryptocurrencies from prior experiments feature again - HOT is the 3rd highest anomaly score for both log returns extreme values and breaks across time; NEXO and XEM are the second and third most anomalous cryptocurrencies across time with respect to structural breaks in variance; and MKR and DGB are the second and third most anomalous after the aforementioned BCD with respect to variance extremes. That is, we see consistent repetition in the cryptocurrencies that behave inconsistently between extreme and erratic behaviours and also were most affected across time by COVID-19.

4. Conclusion

In this paper, we have developed new methods for the study of extreme and erratic behaviours of time series, both individually and in collections. Our work applies and extends the new distance measures between finite sets proposed in [34], and introduces inconsistency matrices and anomaly scores for identification of inconsistent elements under the consideration of multiple types of behaviour and over time.

Applied to the cryptocurrency market, we have uncovered several insights and dissimilarities when studying the various behaviour patterns of returns and variance. In general, cryptocurrency behaviour is more similar in variance than returns, both before and during the pandemic. Before COVID-19, the cryptocurrency market exhibited considerable homogeneity with respect to the structural breaks in variance of individual stocks. This was significantly disrupted by the pandemic, with a reduction in self-similarity, reflected in the Frobenius norms considered, and the emergence of anomalies in hierarchical clustering. COVID-19 also had an impact on the return extremes, with a surprising shift towards positive average means among the return distribution extremities. Relatively little impact on the structural breaks in returns was observed.

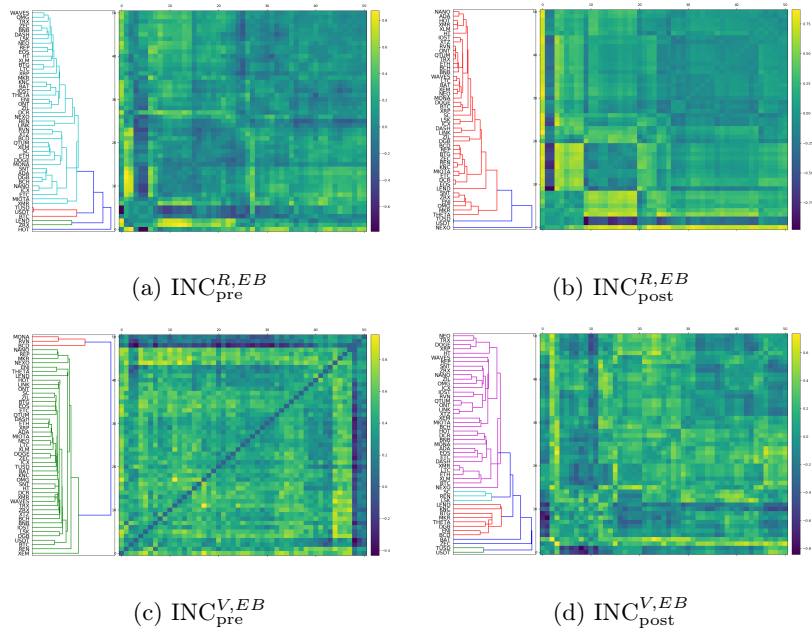


Figure 5: Hierarchical clustering of inconsistency matrices between extreme and erratic behaviour for (a) log returns pre-COVID-19 (b) log returns post-COVID-19 (c) Parkinson variance pre-COVID-19 (d) Parkinson variance post-COVID-19.

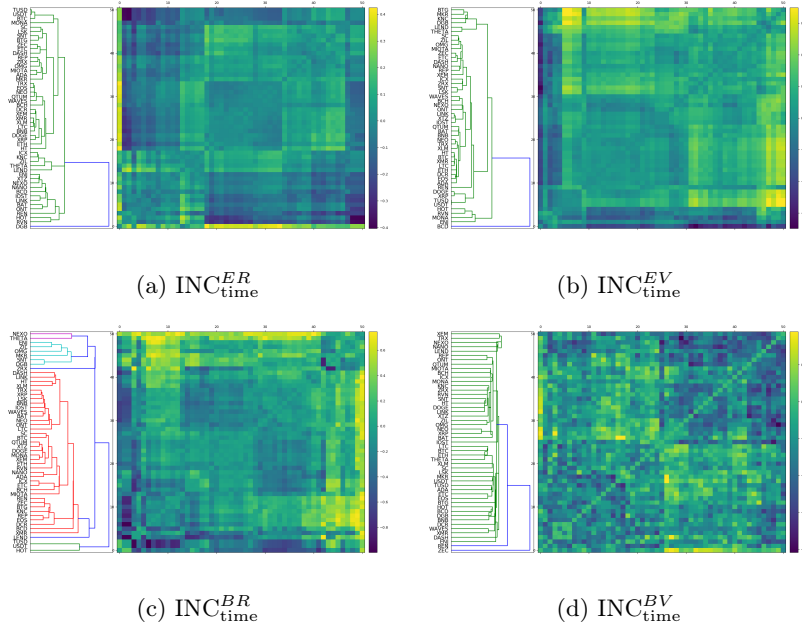


Figure 6: Hierarchical clustering of time inconsistency matrices for (a) log returns extremes (b) Parkinson variance extremes (c) log returns structural breaks (d) Parkinson variance breaks.

Our analysis highlights several notable anomalies in extreme and erratic behaviour over time, most notably, USDT and TUSD. Both cryptocurrencies exhibit unusually docile profiles for extreme and erratic behaviours, likely due to their thin trading structure and lack of market liquidity. Excluding these, several cryptocurrencies repeatedly appeared to be anomalous with respect to behaviour and time, including HOT, NEXO, MKR and XEM, each of which features in the top 3 anomaly scores for at least one inconsistency matrix with respect to time and behaviour.

The precise methodology and applications described in this paper are not an exhaustive representation of the utility of this method. These methods could be used to study structure and identify anomalies among collections of time series in other applications within nonlinear dynamics and with respect to aspects of nonlinearity other than the extreme and erratic behaviour analysed in this paper.

Acknowledgements

Many thanks to Kerry Chen for helpful comments and edits.

Appendix A. Glossary

We include Tables A.3 and A.4, glossaries of cryptocurrency tickers and mathematical objects introduced in this paper, respectively.

Cryptocurrency tickers and names			
Ticker	Coin Name	Ticker	Coin Name
BTC	Bitcoin	DGB	DigiByte
ETH	Ethereum	ZRX	0x
USDT	Tether	KNC	Kyber Network
XRP	XRP (Ripple)	OMG	OMG Network
BCH	Bitcoin Cash	THETA	THETA
LTC	Litecoin	REP	Augur
BNB	Binance Coin	ZIL	Ziliqa
EOS	EOS	BTG	Bitcoin Gold
ADA	Cardano	DCR	Decred
XTZ	Tezos	ICX	ICON
LINK	Chainlink	QTUM	Qtum
XLM	Stellar	LEND	Aave
XMR	Monero	TUSD	TrueUSD
TRX	Tron	BCD	Bitcoin Diamond
HT	Huobi Token	ENJ	Enjin Coin
NEO	NEO	LSK	Lisk
ETC	Ethereum Classic	REN	Ren
DASH	Dash	NANO	Nano
MIOTA	IOTA	RVN	Ravencoin
ZEC	Zcash	SC	Syscoin
MKR	Maker	WAVES	Waves
ONT	Ontology	MONA	MonaCoin
BAT	Basic Attention Token	NEXO	Nexo
XEM	NEM	HOT	Holo
DOGE	Dogecoin	IOST	IOST
SNT	Status		

Table A.3: Cryptocurrency tickers and names

Mathematical objects glossary	
Object	Description
D^{ER}	Distance matrix between return extremes
D^{EV}	Distance matrix between variance extremes
D^{BR}	Distance matrix between return structural breaks
D^{BV}	Distance matrix between variance structural breaks
$A^{ER}, A^{EV}, \text{ etc}$	Corresponding affinity matrices
$\ \mathbf{R}_t\ $	Time varying log return Frobenius vector norm
$\ \Sigma_t\ $	Time varying variance Frobenius vector norm
$\ D^{BR}\ $	Frobenius matrix norm
$INC_{pre}^{R,EB}$	Pre-COVID-19 returns behaviour inconsistency matrix
$INC_{post}^{R,EB}$	Post-COVID-19 returns behaviour inconsistency matrix
$INC_{pre}^{V,EB}$	Pre-COVID-19 variance behaviour inconsistency matrix
$INC_{post}^{V,EB}$	Post-COVID-19 variance behaviour inconsistency matrix
INC_{time}^{ER}	Return extremes time inconsistency matrix
INC_{time}^{EV}	Variance extremes time inconsistency matrix
INC_{time}^{BR}	Return structural breaks time inconsistency matrix
INC_{time}^{BV}	Variance structural breaks time inconsistency matrix

Table A.4: Mathematical objects and definitions

References

- [1] G. Wang, Y. Zhang, J. Zhao, J. Zhang, F. Jiang, Mitigate the effects of home confinement on children during the COVID-19 outbreak, *The Lancet* 395 (2020) 945–947. doi:10.1016/s0140-6736(20)30547-x.
- [2] M. Chinazzi, et al., The effect of travel restrictions on the spread of the 2019 novel coronavirus (COVID-19) outbreak, *Science* (2020) eaba9757. doi:10.1126/science.aba9757.
- [3] Y. Liu, A. A. Gayle, A. Wilder-Smith, J. Rocklöv, The reproductive number of COVID-19 is higher compared to SARS coronavirus, *Journal of Travel Medicine* 27 (2020). doi:10.1093/jtm/taaa021.
- [4] Y. Fang, Y. Nie, M. Penny, Transmission dynamics of the COVID-19 outbreak and effectiveness of government interventions: A data-driven analysis, *Journal of Medical Virology* 92 (2020) 645–659. doi:10.1002/jmv.25750.
- [5] P. Zhou, et al., A pneumonia outbreak associated with a new coronavirus of probable bat origin, *Nature* 579 (2020) 270–273. doi:10.1038/s41586-020-2012-7.
- [6] J. Dehning, J. Zierenberg, F. P. Spitzner, M. Wibral, J. P. Neto, M. Wilczek, V. Priesemann, Inferring change points in the spread of COVID-19 reveals

- the effectiveness of interventions, *Science* 369 (2020) eabb9789. doi:10.1126/science.abb9789.
- [7] F. Jiang, L. Deng, L. Zhang, Y. Cai, C. W. Cheung, Z. Xia, Review of the clinical characteristics of coronavirus disease 2019 (COVID-19), *Journal of General Internal Medicine* 35 (2020) 1545–1549. doi:10.1007/s11606-020-05762-w.
- [8] Z. Y. Zu, M. D. Jiang, P. P. Xu, W. Chen, Q. Q. Ni, G. M. Lu, L. J. Zhang, Coronavirus disease 2019 (COVID-19): A perspective from china, *Radiology* (2020) 200490. doi:10.1148/radiol.2020200490.
- [9] G. Li, E. D. Clercq, Therapeutic options for the 2019 novel coronavirus (2019-nCoV), *Nature Reviews Drug Discovery* 19 (2020) 149–150. doi:10.1038/d41573-020-00016-0.
- [10] L. Zhang, Y. Liu, Potential interventions for novel coronavirus in china: A systematic review, *Journal of Medical Virology* 92 (2020) 479–490. doi:10.1002/jmv.25707.
- [11] M. Wang, R. Cao, L. Zhang, X. Yang, J. Liu, M. Xu, Z. Shi, Z. Hu, W. Zhong, G. Xiao, Remdesivir and chloroquine effectively inhibit the recently emerged novel coronavirus (2019-nCoV) in vitro, *Cell Research* 30 (2020) 269–271. doi:10.1038/s41422-020-0282-0.
- [12] B. Cao, et al., A trial of Lopinavir-Ritonavir in Covid-19, *New England Journal of Medicine* 382 (2020) e68. doi:10.1056/nejmc2008043.
- [13] L. Corey, J. R. Mascola, A. S. Fauci, F. S. Collins, A strategic approach to COVID-19 vaccine r&d, *Science* 368 (2020) 948–950. doi:10.1126/science.abc5312.
- [14] S. Khajanchi, K. Sarkar, Forecasting the daily and cumulative number of cases for the COVID-19 pandemic in india, *Chaos: An Interdisciplinary Journal of Nonlinear Science* 30 (2020) 071101. doi:10.1063/5.0016240.
- [15] C. Manchein, E. L. Brugnago, R. M. da Silva, C. F. O. Mendes, M. W. Beims, Strong correlations between power-law growth of COVID-19 in four continents and the inefficiency of soft quarantine strategies, *Chaos: An Interdisciplinary Journal of Nonlinear Science* 30 (2020) 041102. doi:10.1063/5.0009454.
- [16] M. H. D. M. Ribeiro, R. G. da Silva, V. C. Mariani, L. dos Santos Coelho, Short-term forecasting COVID-19 cumulative confirmed cases: Perspectives for brazil, *Chaos, Solitons & Fractals* 135 (2020) 109853. doi:10.1016/j.chaos.2020.109853.
- [17] T. Chakraborty, I. Ghosh, Real-time forecasts and risk assessment of novel coronavirus (COVID-19) cases: A data-driven analysis, *Chaos, Solitons & Fractals* 135 (2020) 109850. doi:10.1016/j.chaos.2020.109850.

- [18] C. Anastassopoulou, L. Russo, A. Tsakris, C. Siettos, Data-based analysis, modelling and forecasting of the COVID-19 outbreak, *PLOS ONE* 15 (2020) e0230405. doi:10.1371/journal.pone.0230405.
- [19] N. James, M. Menzies, Cluster-based dual evolution for multivariate time series: Analyzing COVID-19, *Chaos: An Interdisciplinary Journal of Nonlinear Science* 30 (2020) 061108. doi:10.1063/5.0013156.
- [20] D. Zhang, M. Hu, Q. Ji, Financial markets under the global pandemic of COVID-19, *Finance Research Letters* (2020) 101528. doi:10.1016/j.frl.2020.101528.
- [21] Q. He, J. Liu, S. Wang, J. Yu, The impact of COVID-19 on stock markets, *Economic and Political Studies* (2020) 1–14. doi:10.1080/20954816.2020.1757570.
- [22] A. Zaremba, R. Kizys, D. Y. Aharon, E. Demir, Infected markets: Novel coronavirus, government interventions, and stock return volatility around the globe, *Finance Research Letters* 35 (2020) 101597. doi:10.1016/j.frl.2020.101597.
- [23] E. Mnif, A. Jarboui, K. Mouakhar, How the cryptocurrency market has performed during COVID 19? A multifractal analysis, *Finance Research Letters* (2020) 101647. doi:10.1016/j.frl.2020.101647.
- [24] J. Chu, S. Nadarajah, S. Chan, Statistical analysis of the exchange rate of bitcoin, *PLOS ONE* 10 (2015) e0133678. doi:10.1371/journal.pone.0133678.
- [25] S. Lahmiri, S. Bekiros, Chaos, randomness and multi-fractality in bitcoin market, *Chaos, Solitons & Fractals* 106 (2018) 28–34. doi:10.1016/j.chaos.2017.11.005.
- [26] D. Kondor, M. Pósfai, I. Csabai, G. Vattay, Do the rich get richer? an empirical analysis of the bitcoin transaction network, *PLoS ONE* 9 (2014) e86197. doi:10.1371/journal.pone.0086197.
- [27] A. F. Bariviera, M. J. Basgall, W. Hasperué, M. Naiouf, Some stylized facts of the bitcoin market, *Physica A: Statistical Mechanics and its Applications* 484 (2017) 82–90. doi:10.1016/j.physa.2017.04.159.
- [28] J. Alvarez-Ramirez, E. Rodriguez, C. Ibarra-Valdez, Long-range correlations and asymmetry in the bitcoin market, *Physica A: Statistical Mechanics and its Applications* 492 (2018) 948–955. doi:10.1016/j.physa.2017.11.025.
- [29] D. Stosic, D. Stosic, T. B. Ludermir, T. Stosic, Multifractal behavior of price and volume changes in the cryptocurrency market, *Physica A: Statistical Mechanics and its Applications* 520 (2019) 54–61. doi:10.1016/j.physa.2018.12.038.

- [30] D. Stosic, D. Stosic, T. B. Ludermir, T. Stosic, Exploring disorder and complexity in the cryptocurrency space, *Physica A: Statistical Mechanics and its Applications* 525 (2019) 548–556. doi:10.1016/j.physa.2019.03.091.
- [31] S. A. Manavi, G. Jafari, S. Rouhani, M. Ausloos, Demythifying the belief in cryptocurrencies decentralized aspects. a study of cryptocurrencies time cross-correlations with common currencies, commodities and financial indices, *Physica A: Statistical Mechanics and its Applications* 556 (2020) 124759. doi:10.1016/j.physa.2020.124759.
- [32] P. Ferreira, L. Kristoufek, E. J. de Area Leão Pereira, DCCA and DMCA correlations of cryptocurrency markets, *Physica A: Statistical Mechanics and its Applications* 545 (2020) 123803. doi:10.1016/j.physa.2019.123803.
- [33] Ş. Telli, H. Chen, Structural breaks and trend awareness-based interaction in crypto markets, *Physica A: Statistical Mechanics and its Applications* 558 (2020) 124913. doi:10.1016/j.physa.2020.124913.
- [34] N. James, M. Menzies, L. Azizi, J. Chan, Novel semi-metrics for multivariate change point analysis and anomaly detection, *Physica D: Nonlinear Phenomena* 412 (2020) 132636. doi:10.1016/j.physd.2020.132636.
- [35] E. del Barrio, E. Giné, C. Matrán, Central limit theorems for the Wasserstein distance between the empirical and the true distributions, *The Annals of Probability* 27 (1999) 1009–1071. doi:10.1214/aop/1022677394.
- [36] G. J. Ross, Parametric and nonparametric sequential change detection in R: the cpm package, *Journal of Statistical Software, Articles* 66 (2015) 1–20. URL: <https://www.jstatsoft.org/v066/i03>. doi:10.18637/jss.v066.i03.
- [37] A. J. Baddeley, Errors in binary images and an L^p version of the Hausdorff metric, *Nieuw Arch. Wisk* 10 (1992) 157–183.